Supramolecular Chemistry
Publication details, including instructions for authors and subscription information:
http://www.informaworld.com/smpp/title~content=t713649759

Sequence-specific recognition and cleavage of DNA by anti-tumour antibiotics

Yukio Sugiura[a]; Le Luo Guan[a]
[a] Institute for Chemical Research, Kyoto University, Uji, Kyoto, Japan

To cite this Article Sugiura, Yukio and Guan, Le Luo(1993) 'Sequence-specific recognition and cleavage of DNA by anti-tumour antibiotics', Supramolecular Chemistry, 1: 3, 313 — 320
To link to this Article: DOI: 10.1080/10610279308035174
URL: http://dx.doi.org/10.1080/10610279308035174

SUPRAMOLECULAR CHEMISTRY, Vol. 1, pp. 313–320
Reprints available directly from the publisher
Photocopying permitted by license only

Sequence-specific recognition and cleavage of DNA by anti-tumour antibiotics

YUKIO SUGIURA* and LE LUO GUAN
Institute for Chemical Research, Kyoto University, Uji, Kyoto 611, Japan

(Received July 26, 1992)

DNA cleavage by a bleomycin–iron complex occurs preferentially at guanine-pyrimidine (5′ → 3′) sequences, in particular at G-C sites. Metallobleomycin binds in the minor groove of B-DNA and the bithiazole moiety probably plays an important role as an anchor on DNA duplex. The 2-amino group of guanine adjacent to the 5′-side of the cleaved pyrimidine base is one key element of the specific 5′-GC recognition by the bleomycin–metal complex. Endiyne anti-tumour antibiotics such as esperamicin A_1 and dynemicin A also interact with the minor groove of DNA, and their strong DNA splitting activity is due to phenylene diradical formation from the enediyne core. A possible binding mode between these antibiotics and B-DNA has been proposed by computer-constructed model building.

INTRODUCTION

Novel anti-tumour antibiotics such as bleomycin, esperamicin A_1, calicheamicin γ_1, neocarzinostatin chromophore and dynemicin A have exceptional anti-tumour potency, unusual chemical structures, and strong DNA cleavage activity (Fig 1). The bleomycin family of glycopeptide antibiotics is used in combination chemotherapy against several types of cancers. The antibiotic requires a metal such as iron(II) and molecular oxygen for its drug action.[1] Oxidative damage of cellular DNA by the metal chelates of bleomycin is believed to be responsible for anti-neoplastic activity. On the other hand, the enediyne family of anti-tumour antibiotics are currently of intense interest.[2] In the presence of reducing agents and DNA, the 'warhead' undergoes a rearrangement to create a phenylene diradical that causes strand cleavage by attacking the sugar groups of the DNA helix. Herein, sequence-specific recognition and cleavage of DNA by these bleomycin and enediyne anti-tumour antibiotics are investigated and discussed.

RESULTS AND DISCUSSION

Increased DNA binding affinity of bleomycin–metal chelation

Apparent DNA binding constants of free bleomycin, the bleomycin–Co(III) complex, and the bleomycin–Zn(II) complex, were evaluated in 10 mM Tris-HCl buffer (pH 7.5) by our previous fluorescence method.[3] Table 1 compares the DNA binding parameters of free bleomycin and its metal complexes. The apparent binding constants for calf thumys DNA and poly d(G-C) of the bleomycin–Co(III) complex are evidently higher than those of free bleomycin or the bleomycin–Zn(II) complex. The binding sites sizes ($n/2$ = 2.52–2.43 base pairs) of the bleomycin–Co(III) complex with calf thymus DNA and poly d(G-C) are smaller than those of free bleomycin (3.56–3.07) and the bleomycin–Zn(II) complex (3.31–2.89), suggesting a more compact conformation of bleomycin–Co(III) complex.

DNase I cleavage-protection analysis (footprinting) for free bleomycin and its metal complexes was performed by the digestion of pBR322 HifI-HhaI (200 base pairs) DNA fragment with DNase I. In contrast to DNase I digestion with free bleomycin and the bleomycin–Zn(II) complex, DNase I digestion with the bleomycin–Co(III) complex obviously gave some DNA footprints. The strong protection regions are detected at the sites containing the 3′-CG sequences as follows:

```
      1020          1030          1040          1050
       |             |             |             |
5′-CCGGCGGCATCGGGATGCCCGCGTTGCAGGCCATGCTG
3′-GGCCGCCGTAGCCCTACGGGCGCAACGTCCGGTACGAC
      [* *] *       [* *] *       [* *]
```

The asterisks (*) represent the bases cleaved by the bleomycin–Co(III)–UV light system. The present difference of DNase I protection among free bleomycin, the bleomycin–Co(III) complex, and the bleomycin–Zn(II) complex appears to reflect stronger affinity and more favourable conformation of the bleomycin–Co(III) complex for B-DNA binding. Levy and Hecht[4] communicated that (1) Cu(II) facilitates bleomycin-mediated unwinding of plasmid DNA and (2) Zn(II) produces no more DNA unwinding than that observed bleomycin alone.

Figure 2 compares circular dichroism (CD) spectra for calf thymus DNA or d(CGCGTACACGCG) interactions with free bleomycin and its *Co(III)*

* To whom correspondence should be addressed.

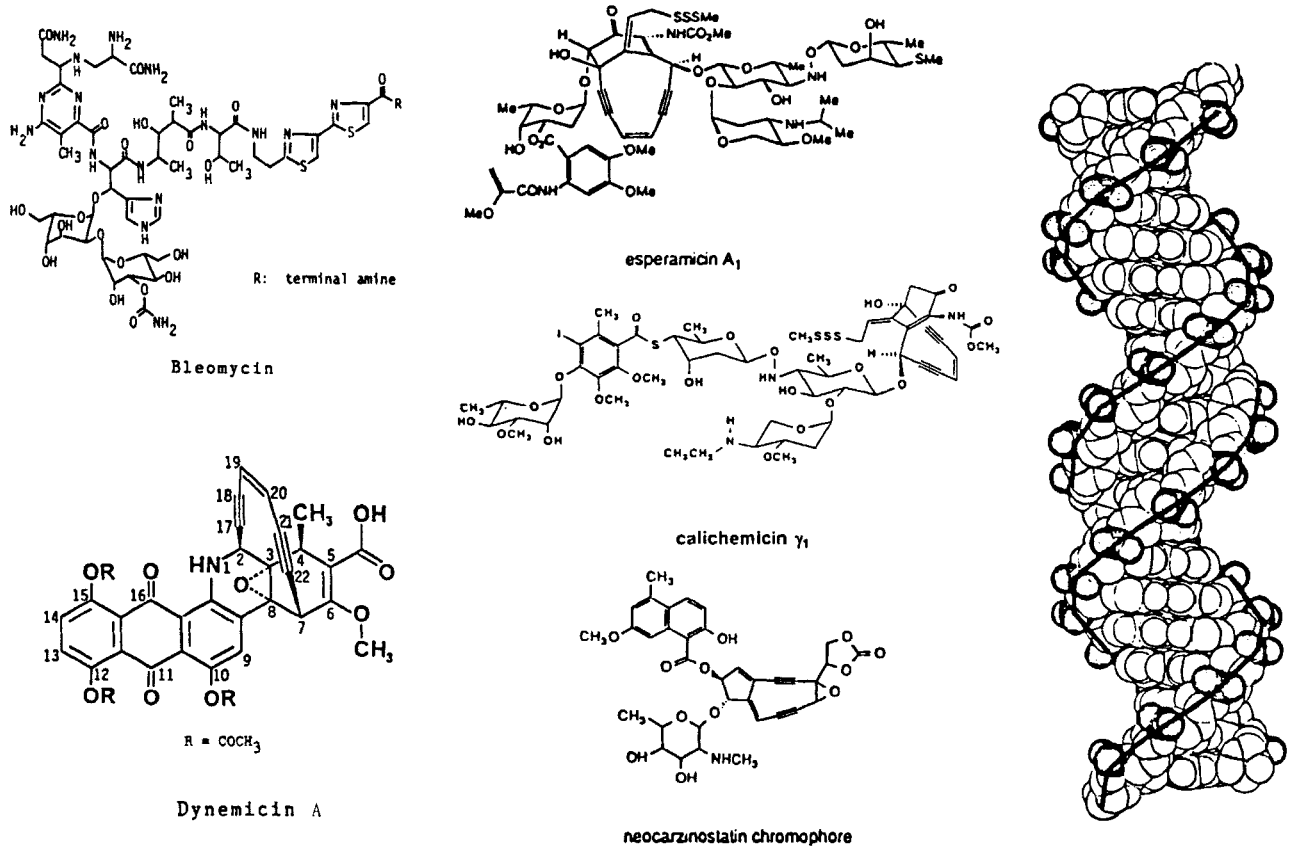

Figure 1 DNA-cleaving anti-tumour antibiotics.

Table 1 Binding parameters of free bleomycin, bleomycin–Co(III) complex, and bleomycin–Zn(II) complex of calf thymus DNA and poly [d(G-C)]

	$K \times 10^4$ (M^{-1})	n (base)
Bleomycin + calf thymus DNA	0.79 ± 0.03	7.11 ± 0.27
Bleomycin–Co(III) + calf thymus DNA	29.8 ± 4.61	5.04 ± 0.38
Bleomycin–Zn(II) + calf thymus DNA	4.24 ± 0.35	6.62 ± 0.21
Bleomycin + poly [d(G-C)]	1.05 ± 0.02	6.13 ± 0.15
Bleomycin–Co(III) + poly [d(G-C)]	36.7 ± 3.70	4.86 ± 0.43
Bleomycin–Zn(II) + poly [d(G-C)]	5.86 ± 0.42	5.77 ± 0.35

complex. Clearly, the CD feature of the bleomycin–Co(III)–DNA complex is distinct from that of free bleomycin–DNA complex. The cobalt chelation probably rearranges free bleomycin into a conformation that facilitates DNA binding. Similar metal-dependent folding has been demonstrated in so-called 'zinc finger' DNA binding motifs.[5] In gene 32 protein, the single-stranded DNA binding protein from bacteriophage T4, it is known that the binding affinity of the Zn(II) protein for poly (dT) is considerably reduced by the removal of Zn(II) ions.[6] The present results indicate that the metal chelation of bleomycin antibiotics significantly participates in increasing the DNA binding affinity of bleomycin, as well as in the previously recognized function of dioxygen binding and activation.[7]

Interaction mode of DNA with metallobleomycin

Bleomycin consists of three components, namely (1) a metal-chelating site of β-aminoalanine-pyrimidine-β-hydroxyhistidine portion, (2) a DNA interaction site of bithiazole-terminal amine moiety, and (3) a gulose-mannose sugar region.[1] The size of approximately three base pairs of the bleomycin–Co(III) complex suggests a compact, folded configuration in metallobleomycin. Indeed, a proton NMR relaxation study of the bleomycin–Mn(II) complex reveals that the bithiazole and terminal amine protons (5.4 and 7.4 Å) are considerably closer to the metal centre.[8] We previously indicated that the bleomycin–Fe(III) complex involves as many as five nitrogenous ligands of the β-aminoalanine-pyrimidine-β-hydroxyhistidine portion with a geometry similar to haeme complexes.[7] The ferric–peroxide complex species of bleomycin is

also known to attack primarily the C'4 protons of cytosine robose at the 5'-GC sequence.[9] In addition, the experimental results of the DNA modifications with distamycin A and anthramycin strongly indicate

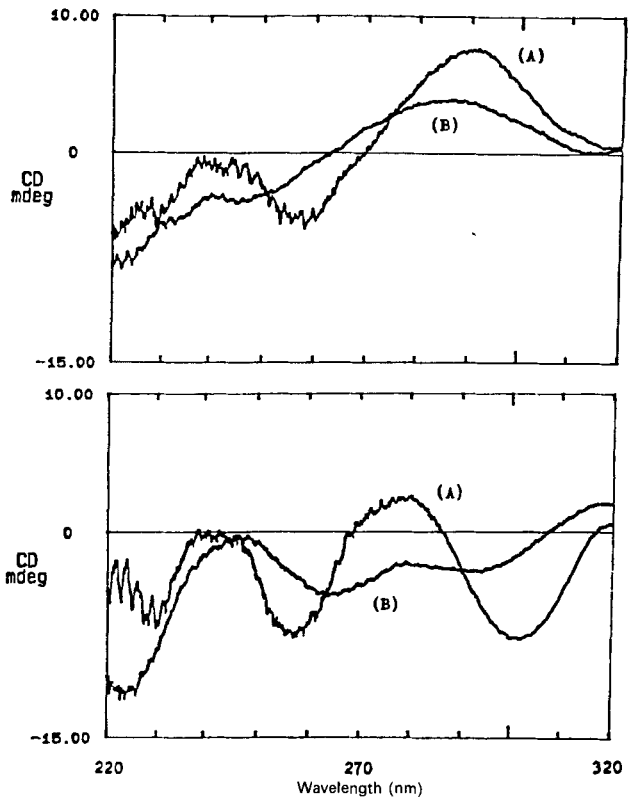

Figure 2 CD spectra for calf thymus DNA (A) and d(CGCGTACG-CGCG) (B) interactions with free bleomycin (upper) and its Co(III) complex (lower) at pH 7.5.

that metallobleomycin binds in the minor groove of B-DNA and that the 2-amino group of the guanine residue plays an important role in DNA–metallobleomycin interactions. By a computer-constructed molecular model, the stereochemical fit of metallobleomycin to duplex DNA was examined on the basis of these experimental data. Figure 3 shows a stereoview of the interaction mode between the bleomycin–metal complex and self-complemenetary d(A-T-G-C-C-A)$_2$. Here, the 5'-TGCC sequence was chosen as the best sequence from the consensus sequence analysis of the DNA breakage by metallobleomycin. The configurations of the nucleic acid fragments and the metal coordination core were taken from the standard B-DNA and X-ray crystallographic data of the bleomycin biosynthetic intermediate P–3A–Cu(II) complex.[10,11] Stereomodels suggest that the conformational structure is composed of the 2-amino group of guanine, the 2-carbonyl oxygen of the pyrimidine base in the 5' guanine-pyrimidine sequence, and the 2-carbonyl oxygen of the cytosine base complementary to the 5-GC and G-CT sequences. This convex environment appears to be profitable for the primary binding of metallobleomycin and is entirely different from the situation in 5'-CG and 5'-TG sequences. In order to achieve specific guanine recognition in the minor groove of DNA, therefore, steric space and a hydrogen bond acceptor for the guanine 2-amino group are probably required from the bleomycin molecule. In our opinion, the guanine recognition by compact, folded metallobleomycin in the minor groove of the 5'-GC sequence can be achieved by a snug fit of the concave face of the bithiazole–carboxamide moiety

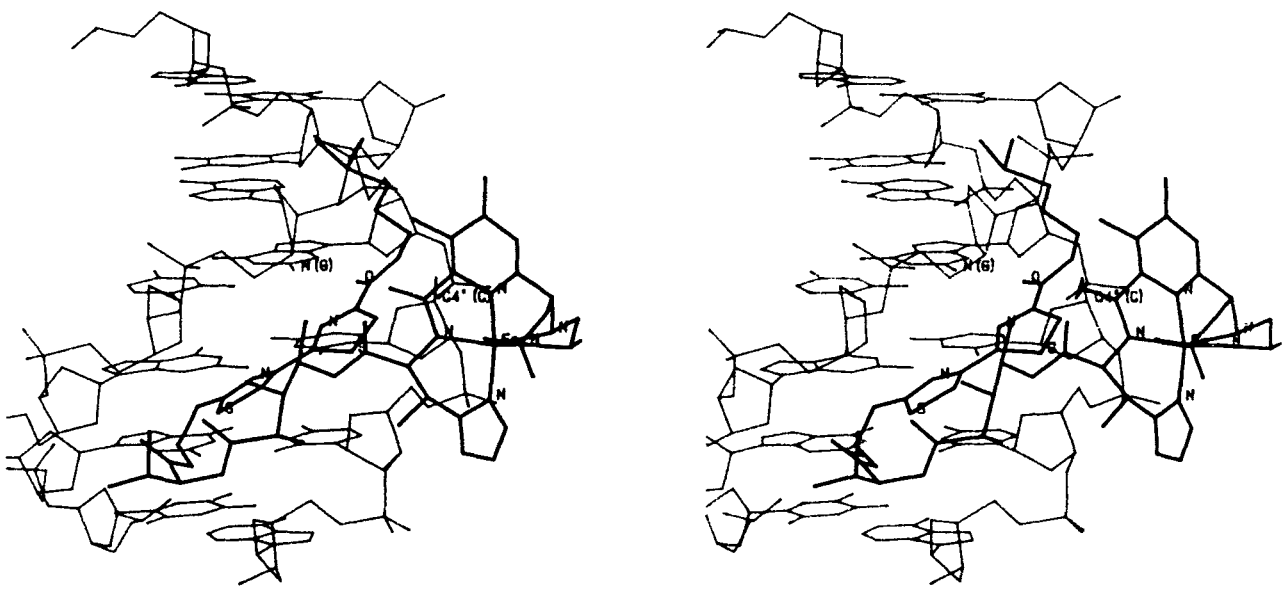

Figure 3 Binding mode of metallobleomycin with d(ATGCCA). Darker and lighter bonds represent metallobleomycin and the deoxyribonucleotide, respectively. (See color plate II at the back of this issue.)

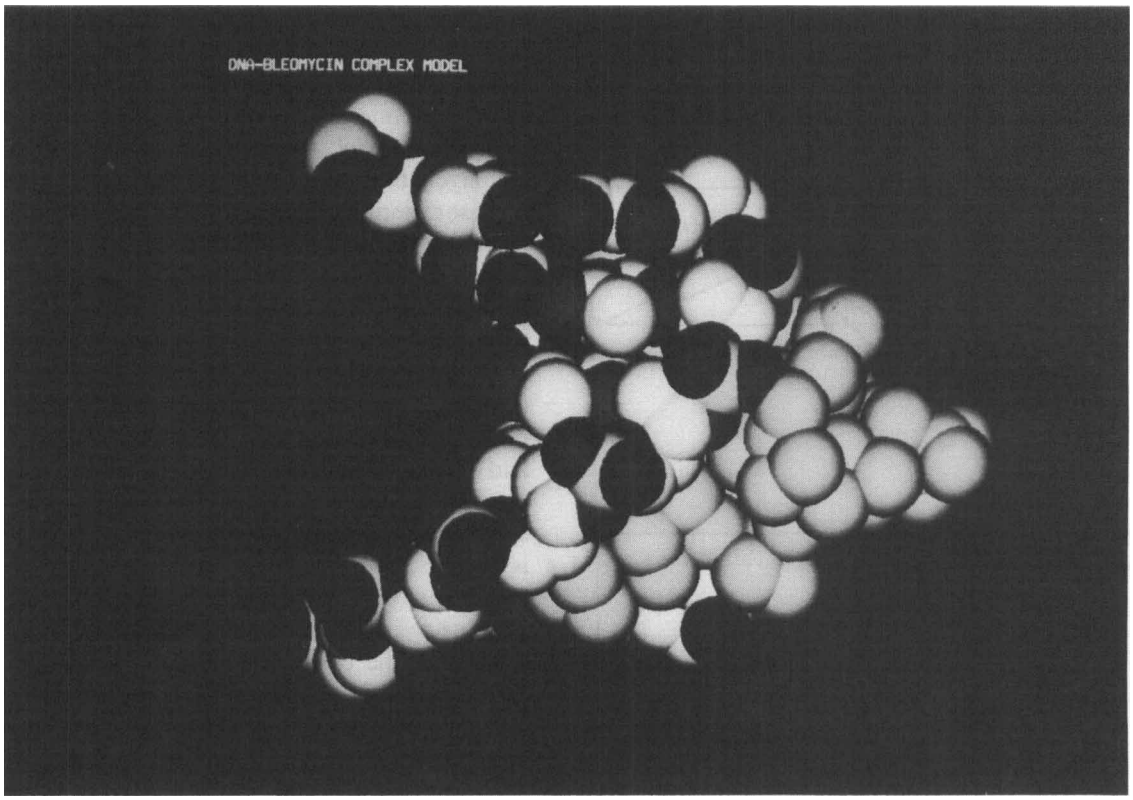

Figure 4 Space-filling molecular model of metallobleomycin in the minor groove interaction of DNA. (See color plate III at the back of this issue.)

and by hydrogen bonds of the guanine 2-amino group with two ring nitrogens of the bithiazole group. The 2-amino group of the guanine base adjacent to the 5′-side of the cleaved pyrimidine base is one key element of specific 5′-GC or 5′-GT recognition by metallobleomycin, and the bithiazole group plays an important role as anchor on B-DNA. The present results indicate that metallobleomycin interacts with DNA duplex as a minor-groove binder rather than an intercalator. Figure 4 shows a space-filling molecular model of metallobleomycin–DNA binding. It is difficult for metallobleomycin to intercalate through its bithiazole moiety between DNA bases because of the structural bulkiness. This situation is evidently different from the proposed intercalative DNA binding of the simple bithiazole model compound alone.

Characteristics of DNA cleavage by esperamicin and dynemicin antibiotics

Esperamicin attacked preferentially at T and C bases in oligopyrimidine regions such as 5′-CTC, 5′-TTC, and 5′-TTT (see Fig 5). The sequence-specific cleavage mode of esperamicin A_1 is significantly affected by pretreatment of DNA with netropsin and distamycin A, suggesting that interaction of esperamicin A_1 occurs through the minor groove of B-DNA.[12] This was further supported by the asymmetric cleavage pattern

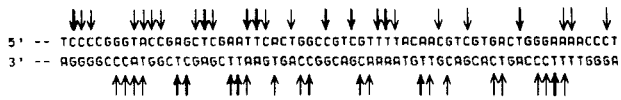

Figure 5 DNA cleavage sites of esperamicin A_1. Arrows and their thicknesses indicate the cutting sites and the relative intensity of the bands, respectively.

to the 3′-side on the opposite strand of DNA. Although the cleavage of DNA by esperamicin A_1 was greatly accelerated in the presence of thiol compounds, DNA strand scission by dynemicin A was significantly enhanced by the addition of NADPH or thiol compounds. The preferential scission site of dynemicin A was on the 3′-side of purine bases such as 5′-GC, 5′-GT, and 5′-AG sequences and was clearly different from the cleavage sites of esperamicin A_1.[13] Dynemicin A-mediated DNA cleavage was strongly inhibited by pretreatment of DNA with distamycin A and anthramycin. The result also indicates the interaction of dynemicin A in the minor groove of the DNA duplex.

Interaction modes of B-DNA with esperamicin A_1 and dynemicin A

Of special interest is the fact that esperamicin A_1 and three products of hydrolysis of the glycon, esperamicins C, D, and E, were found to retain a common pyrimidine sequence selectivity in the DNA cleavage.

Here, esperamicin C lacks both L-fucose and the anthranilate moieties from esperamicin A_1. Esperamicin D is similar to esperamicin C but also lacks the thiosugar moiety, and esperamicin E has the enediyne core and only one sugar moiety. The results strongly suggest that the diacetylenic ring core itself determines the sequence specificity for strand scission of duplex DNA by esperamicin antibiotics. Recent synthesized model compounds also reveal that the enediyne core is an important element for base recognition.[14] The sugar residues appear to exert a strong influence on cleavage efficiency, presumably by interacting non-specifically with DNA.

It is known that the enediyne moiety is the key functional group for DNA cleavage by esperamicin A_1. The mechanism by which esperamicin degrades DNA has been suggested to involve bioreductive cleavage of the allylic trisulphide and Michael addition of the resultant thiolate to the neighbouring bridgehead olefin, followed by enediyne cyclization to give a phenylene diradical.[12] Therefore, the first step of DNA cleavage in the minor groove is abstraction of a C-5′ proton from the deoxyribose backbone by the C-4 carbon radical of the phenylene diradical produced from the enediyne core. Recently, we found that esperamicin C gives the DNA splitting mode close to calicheamicin γ_1 rather than esperamicin A_1. Probably, the deoxyfucose-anthranilate moiety of esperamicin A_1 contributes to steric hinderance for hydrogen abstraction from C-1′ or C-4′ of deoxyribose by the C-1 carbon radical of the phenylene diradical (Fig 6). At the present stage, Figure 7 demonstrates a preliminary computer-constructed model building for a possible binding mode of esperamicin A_1 to the DNA double helix. Especially, the enediyne core is situated in the minor groove of DNA.

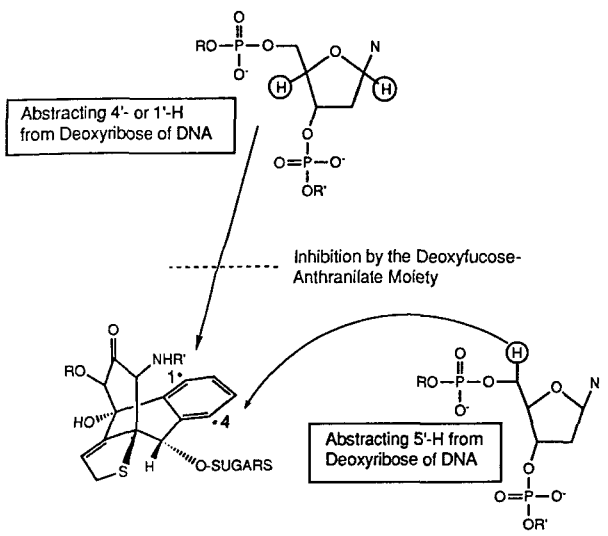

Figure 6 DNA cleaving modes by esperamicin antibiotics.

For dynemicin A, opening of the epoxide ring is the key to its activation to form the diaryl radical form of dynemicin A, namely DNA-cleaving intermediate. A more reasonable proposal of the mechanism for epoxide ring opening requires the conversion of dynemicin A by a 1 electron reduction or two sequential 1 electron reductions to the hydroquinone. Presumably, a phenylene diradical produced by cyclization of the endiyne core is the active species of dynemicin A, similar to the mechanism proposed for compounds in this class of anti-tumour agents responsible for potent DNA cleavage.[15] Intercalation of the anthraquinone ring into the DNA duplex followed by attack of the phenylene diradical formed from the enediyne core is considered as a possible mechanism of dynemicin action. Our results indicate that dynemicin A abstracts the C-1′ hydrogen of DNA deoxyribose and that the damaged DNA leads to strand breaks with the formation of 5′- and 3′-phosphate termini. The lesions of C-4′ hydrogen also occur at the 3′-side of GC base pairs such as 5′-CT and 5′-GA, leading to 5′-phosphate and 3′-phosphoglycolate termini or 4′-hydroxylated abasic sites. Figure 8 shows a preliminary computer-constructed model of dynemicin A–DNA interaction. Finally, we must determine NMR and X-ray crystallographic studies for the specific enediyne drug-duplex DNA interaction.

EXPERIMENTAL SECTION

Drugs and chemicals

Peplomycin supplied by Nippon Kayaku was used as the bleomycin ligand in this study. After equimolar $Co(NO_3)_2$ and bleomycin, the green-coloured bleomycin–Co(III) complex species was isolated by preparative HPLC.[16] Esperamicin and dynemicin antibiotics were gifts of Bristol–Meyers Squibb. DNase I and restriction enzymes were obtained from Takara Shuzo (Kyoto, Japan), and all other chemicals used were of commercial reagent grade.

Estimation of DNA binding affinity

In 10 mM Tris-HCl buffer (pH 7.5), apparent binding constants between metallobleomycin (or free bleomycin) and DNAs were evaluated by a fluorescence-quenching method similar to that of Chien *et al.*[17] The experimental data were analysed by the neighbour-exclusion model of McGhee and von Hippel.[18] Binding parameters, K (M^{-1}) and n (base), obtained from non-linear least-squares fitting, indicated the apparent binding constant and number of bases per binding site, respectively.

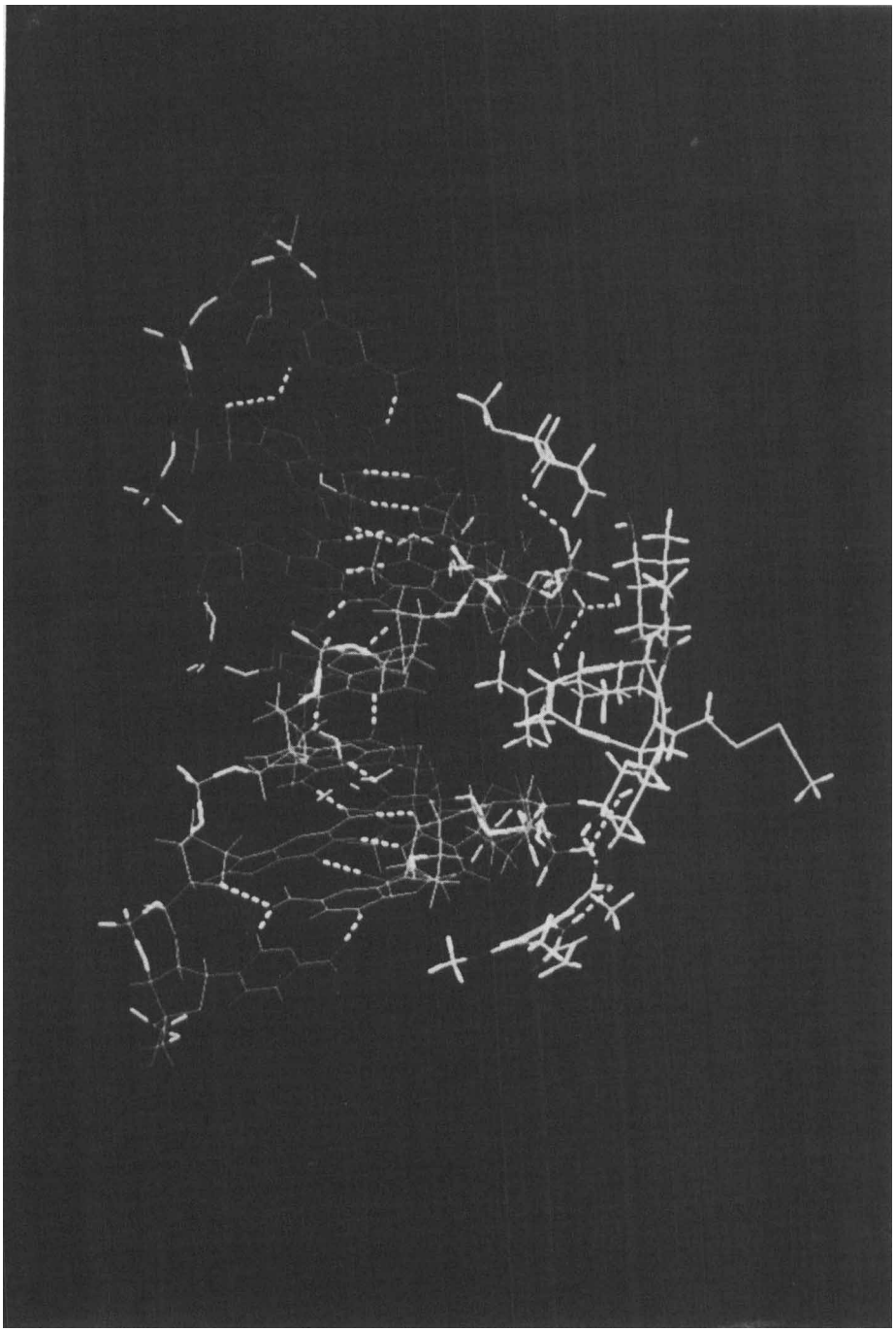

Figure 7 Computer-constructed model of esperamicin A_1–DNA binding. (See color plate IV at the back of this issue.)

Preparation of ^{32}P-labelled DNA fragments

The adequate restriction fragments were used in this study, and the number is used from the genomic numbering system of pBR322 DNA. [α-^{32}P]dTTP and [γ-^{32}P]ATP were utilized for 3′- and 5′-end labellings, respectively. DNA sequencing was carried out by the Maxam–Gilbert method.[19] Densitometric analysis of the autoradiogram was performed with a Bio-Rad 1650-II scanning densitometer.

DNase I footprinting

The reaction mixture contained the singly end-labelled fragment, sonicated calf thymus DNA (500 μM), and the antibiotic, in 10 mM Tris-HCl buffer (pH 7.5). After pre-incubation at 37°C for 30 min, the sample was digested with DNase I (final concentration, 0.5 μg/ml) for 4 min. The reaction was stopped by adding NaOH-adjusted Na_2EDTA, and then the sample was lyophilized.

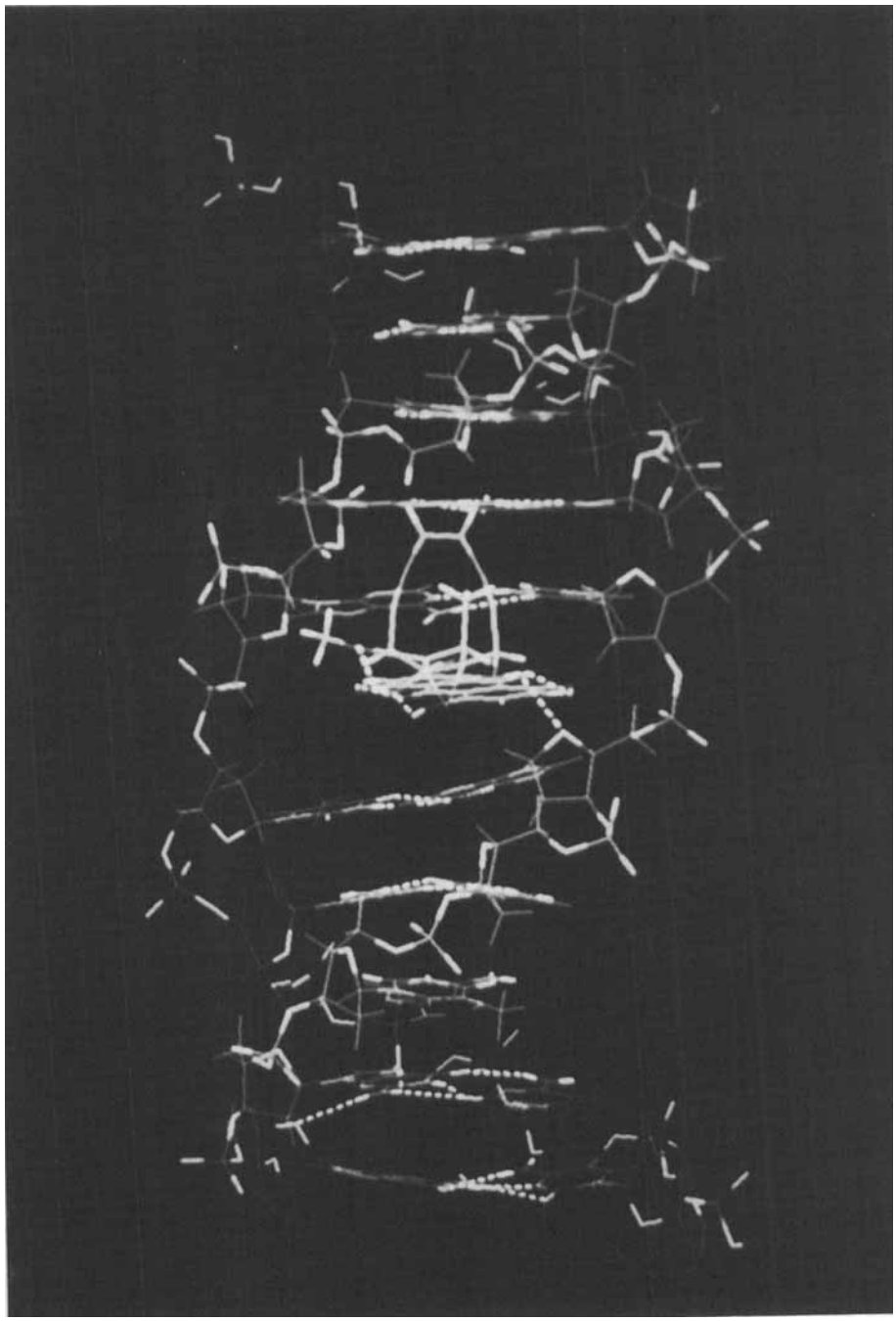

Figure 8 Computer-constructed model of dynemicin A–DNA binding. (See color plate V at the back of this issue.)

Nucleotide sequence analysis

The nucleotide sequence cleavage was initiated by addition of the antibiotic, and then the samples were incubated at 37°C for 15 min. Cold ethanol was added to the sample solutions in order to stop the reaction. Electrophoresis was performed in a 10% polyacrylamide/7 M urea slab gel at 1500 V for 4 h.

Computer graphic modelling

The stereochemical fit of the antibiotics in duplex DNA was examined by inspection of a computer-constructed and energy-minimized molecular model using a Frodo program[20] on an Evans and Sutherlands multipicture system.

ACKNOWLEDGMENT

We thank Drs. S. Imajo and M. Ishiguro (Suntory Biomedical Institute) for pertinent advice on computer graphic modellings. This study was supported in part by Grant-in-Aid for Scientific Research on a Priority

Area from the Ministry of Education, Science and Culture, Japan.

REFERENCES

1 Sugiura, Y.; Takita, T.; Umezawa, H.; in *Metal Ions in Biological Systems*, Sigel, H. (Ed.), Marcel Dekker, New York, **1985**, p. 81.
2 Bicolaou, K.C.; Dai, W.-M.; *Angew. Chem. Intl. Ed. Engl.* **1991**, *30*, 1387.
3 Kuwahara, J.; Sugiura, Y.; *Proc. Natl. Acad. Sci. USA*, **1988**, *85*, 2459.
4 Levy, M.L.; Hecht, S.M.; *Biochemistry* **1988**, *27*, 2647.
5 Berg, J.M.; *Proc. Natl. Acad. Sci. USA* **1988**, *85*, 99.
6 Giedroc, D.P.; Keating, K.M.; Williams, K.R.; Konigsberg, W.H.; Coleman, J.E.; *Proc. Natl. Acad. Sci. USA* **1986**, *83*, 8452.
7 Sugiura, Y.; *J. Am. Chem. Soc.* **1980**, *102*, 5208.
8 Sheridan, R.P.; Gupta, R.K.; *J. Biol. Chem.* **1981**, *256*, 1242.
9 Stubbe, J.; Kozarich, J.W.; *Chem. Rev.* **1987**, *87*, 1107.
10 Arnott, S.; Campbell-Smith, P.; Chandrasekaran, R.; in *CRC Handbook of Biochemistry*, Vol. 2 (Fasman, C.D., ed.), CRC, Cleveland, **1976**, p. 411.
11 Iitaka, Y.; Nakamura, H.; Nakatani, T.; Muraoka, Y.; Fujii, A.; Takita, T.; Umezawa, H.; *J. Antibiot.* **1978**, *31*, 1070.
12 Sugiura, Y.; Uesawa, Y.; Takahashi, Y.; Kuwahara, J.; Golik, J.; and Doyle, T.W.; *Proc. Natl. Acad. Sci. USA* **1989**, *86*, 7672.
13 Sugiura, Y.; Shiraki, T.; Konishi, M.; Oki, T.; *Proc. Natl. Acad. Sci. USA*, **1990**, *87*, 3831.
14 Hirama, M.; Gomibuchi, T.; Fujiwara, K.; Sugiura, Y.; Uesugi, M.; *J. Am. Chem. Soc.* **1991**, *113*, 9851.
15 Sugiura, Y.; Arakawa, T.; Uesugi, M.; Shiraki, T.; Ohkuma, H.; Konishi, M.; *Biochemistry* **1991**, *30*, 2989.
16 Chang, C.-H.; Dallas, J.L.; Meares, C.F.; *Biochem. Biophys. Res. Commun.* **1983**, *110*, 959.
17 Chien, H.; Grollman, A.P.; Horwitz, S.B.; *Biochemistry* **1977**, *16*, 3641.
18 McGhee, J.D.; von Hippel, P.H.; *J. Mol. Biol.* **1974**, *86*, 469.
19 Maxam, A.M.; Gilbert, W.; *Methods Enzymol.* **1980**, *65*, 499.
20 Jones, T.A.; *J. Appl. Crystallogr.* **1978**, *11*, 268.